Research Square

Preprints are preliminary reports that have not undergone peer review.
They should not be considered conclusive, used to inform clinical practice,
or referenced by the media as validated information.

Ferric carboxymaltose has a higher distribution into myocardium than gadobutrol assessed by quantitative T1 mapping in healthy volunteers

Goran Abdula

goran.abdula@ki.se

Karolinska University Hospital, and Karolinska Institutet

Magnus Lundin

Karolinska University Hospital, and Karolinska Institutet

Jannike Nickander

Karolinska University Hospital, and Karolinska Institutet

Peder Sörensson

Karolinska University Hospital, and Karolinska Institutet

Andreas Sigfridsson

Karolinska University Hospital, and Karolinska Institutet

Raquel Themudo

Karolinska University Hospital in Huddinge

Martin Ugander

Kolling Institute

Research Article

Keywords: Ferric carboxymaltose, Cardiovascular magnetic resonance imaging, T1 mapping, Myocardial iron, Partition coefficient, Gadolinium.

Posted Date: November 24th, 2026

DOI: https://doi.org/10.21203/rs.3.rs-11677806/v1

License: This work is licensed under a Creative Commons Attribution 4.0 International License.
Read Full License

Additional Declarations: No competing interests reported.

Ferric carboxymaltose has a higher distribution into myocardium than gadobutrol assessed by quantitative T1 mapping in healthy volunteers

Goran Abdula MD PhD[1], Magnus Lundin MD PhD[1], Jannike Nickander MD PhD[1],

Peder Sörensson MD PhD[4], Andreas Sigfridsson, PhD[1], Raquel Themudo MD PhD[2,3], Martin Ugander MD PhD[1,5]

[1]Department of Clinical Physiology, Karolinska University Hospital, and Karolinska Institutet, Stockholm, Sweden
[2] Department of Radiology, Karolinska University Hospital in Huddinge, Stockholm, Sweden
[3] Division of Medical Imaging and Technology, Department of Clinical Science, Intervention and Technology (CLINTEC), Karolinska Institute/Karolinska University Hospital, Stockholm, Sweden
[4]Department of Cardiology, Karolinska Institutet and Karolinska University Hospital, Solna, Stockholm
[5]Kolling Institute, Royal North Shore Hospital, and University of Sydney, Sydney, Australia

Corresponding author:

Goran Abdula, MD, PhD, Department of Clinical Physiology, Karolinska University Hospital and Karolinska Institute, Stockholm, Sweden

E-mail: goran.abdula@ki.se

Phone: +46707408385

Abstract

Ferric carboxymaltose (FCM) improves symptoms, functional capacity and clinical outcomes in patients with heart failure, regardless of ejection fraction or anemia status. We aimed to evaluate and quantify the dynamic tissue distribution of FCM using cardiovascular magnetic resonance (CMR).

This prospective, single-center study was part of the Iron-CMR trial (EudraCT: 2014-002455-26). T1 mapping was performed both pre- and post-contrast to assess relative changes in T1 and the partition coefficient (λ) in myocardium, liver, spleen and skeletal muscle up to 60 minutes after onset of a 15-minute infusion of 20 ml (50 mg iron/ml) FCM in healthy male volunteers. Myocardial λ was compared with that of gadobutrol (0.2 mmol/kg) in an age-matched cohort. Groups were compared using Mann-Whitney U test. Twenty-five healthy males (age 27±3 years) underwent CMR with intravenous FCM (n=8) or gadobutrol (n=17). T1 decreased in the myocardium, blood, liver, spleen and skeletal muscle following FCM infusion ($p < 0.001$ for all). FCM λ remained relatively constant in the myocardium and spleen (65±2% and 81±20%, respectively, at 30 minutes), whereas λ increased in the liver and skeletal muscle. Myocardial λ was significantly higher for FCM than gadobutrol (65±2vs 42±1%, $p < 0.0001$). CMR T1 mapping enables detection and quantification of the dynamic tissue distribution of FCM in the myocardium, liver, spleen, and skeletal muscle. The higher myocardial λ for FCM compared with gadobutrol suggests greater myocardial distribution than extracellular contrast agents, most likely due to additional distribution into the intracellular space.

Keywords

Ferric carboxymaltose, Cardiovascular magnetic resonance imaging, T1 mapping, Myocardial iron, Partition coefficient, Gadolinium.

Introduction

Iron deficiency is a common comorbidity in patients with heart failure [1]. Ferric carboxymaltose (FCM) is an intravenous iron preparation which enables controlled release of non-ionic iron within the cells into the serum under physiological conditions [2]. Studies reveal that treatment with intravenous FCM in patients with heart failure and iron deficiency improves clinical symptoms and functional capacity [3] even in those with preserved ejection fraction (HFpEF) [4], and decreases hospital admissions regardless of the presence of anemia [5; 6]. This observation suggests that iron deficiency has a pathophysiological mechanism beyond anemia that contributes to heart failure. Myocardial iron deficiency has been suggested to have a role in the development of heart failure [7]. Therefore, the ability to non-invasively quantify myocardial iron uptake is of considerable clinical interest, since the pathological consequences of iron deficiency are potentially reversible.

The current non-invasive reference method for quantification of myocardial iron relies on using magnetic resonance imaging to measure T2*. At 1.5T scanner the normal myocardial T2* is typically 37±5 ms. However, a threshold of 20 ms, corresponding to double the amount of myocardial iron than normal [8], has been used because T2* at low iron levels is sensitive to non-iron influences, such as motion and susceptibility artefacts [9]. It has been demonstrated that T1 mapping can be used to quantify iron concentrations [10] and showed that intravenous FCM administration in patients with heart failure significantly reduced myocardial T1 values [11-13]. In addition, T1 mapping has the potential to detect milder degrees of myocardial iron overload compared to T2* [14]. Approximately one third of subjects with low myocardial T1, secondary to iron overload in the myocardium, had normal T2* values (>20 ms) [14]. Furthermore, myocardial T1 mapping methods are less prone to image artifacts compared to T2* sequences [15]. Post-contrast T1 mapping has been used to quantify gadolinium-based contrast agent concentration over time [16; 17], and its distribution volume in the myocardium [18]. Pre- and postcontrast T1 measurements have been used to calculate the blood-tissue partition coefficient, lambda (λ), for gadolinium-based contrast agents [19]. However, T1 mapping has not been used to quantify changes in tissue iron content in vivo after intravenous administration of iron.

Therefore, the purpose of this study was to evaluate the use of T1 mapping to detect and quantify myocardial iron distribution of FCM, a clinically available intravenous iron substitution agent, and to compare the myocardial distribution of FCM to that of the extracellular gadolinium-based contrast agent gadobutrol. We hypothesized that T1 mapping can be used to detect and quantify iron uptake in the myocardium.

Materials and methods

This study is a prospective exploratory imaging study of healthy male volunteers that received ethics approval from the Stockholm Regional Board of Ethics (application number 2014/1140-31/3). All subjects provided written informed consent prior to study enrolment.

Participants. Twenty-five healthy male volunteers aged18 years or older were recruited for the study. Healthy subjects were defined as having no previous history of cardiovascular or systemic disease and a normal resting electrocardiogram. Participants were excluded If the hand a history of any chronic illnesses, cardiac diseases, presence of a pacemaker, claustrophobia, known allergy to either gadolinium-based contrast agent or hypersensitivity to iron products, liver dysfunction, or signs of iron overload.

Eight subjects underwent CMR scan before and after intravenous administration of ferric carboxymaltose (Ferinject®, Vifor Pharma) as a part of prospective single-center Iron-CMR trial (Clinicaltrialsregister.eu registration no. EudraCT: 2014-002455-26). A separate group of seventeen healthy male subjects underwent CMR before and after intravenous administration of gadobutrol (Gadovist®, Bayer AB); this cohort has previously been reported as a part of a larger study [20]. The unequal group sizes reflect the separate recruitment periods and study aims. However, the smaller sample size in the FCM group was considered sufficient to detecting changes in T1 values and partition coefficient, providing 80% statistical power based on effect sizes anticipated from a previous study [21].

Imaging protocol. CMR imaging was performed using a 1.5T scanner (Magnetom Aera, Siemens) with a 32-channel coil. In all subjects, T1 quantification was performed using a Modified Look-Locker Inversion-recovery (MOLLI) sequence. The protocol of a 5(3s)3 sampling scheme was employed for pre-contrast imaging and following intravenous administration of gadobutrol, whereas a 4(1s)3(1s)2 sampling scheme [22] was utilized after intravenous administration of FCM. This variation in MOLLI acquisition schemes reflects historical difference between the two cohorts. T1 maps were reconstructed using inline motion correction [23]. The study population and the main component of CMR protocol used for calculation of FCM and gadobutrol lambda (λ) are outlined in Fig. 1. Typical imaging parameters for MOLLI were: matrix size 144x256, field of view 270x360 mm2, flip angle 35°, TE 2.6 ms, TR 278 ms, parallel acquisition technique (PAT) factor of 2, slice thickness 8 mm, phase encoding lines 125.

T1 maps were acquired prior to the administration of the contrast agent, every 2-3 minutes during the 15-minute-long intravenous infusion of FCM (20 ml, 50 mg iron/ml, Vifor Pharma), and every 5 minutes following completion of infusion up to 60 minutes. In the gadolinium-based contrast agent group (n= 17), T1 maps were acquired before and around 15-20 minutes after intravenous administration of 0.2 mmol/kg of gadobutrol (Bayer AB).

A balanced steady state free precession (bSSFP) cine sequence was acquired covering the left ventricle in a short-axis stack and three long-axis views, in order to calculate left ventricular volumes and function. Typical imaging parameters for cine imaging included: flip angle 57°, pixel size 1.4 mm2, TR/TE 2.4/1.2 ms, matrix size 143x256 mm^2 and field of view 303 x 360 mm2.

Image analysis. No examinations were excluded due to artifacts. However, the regions of interest for each organ were carefully placed to avoid partial volume effect and to minimize the impact of any obvious artifacts within the images. Left ventricular function, volumes and mass were quantified offline using freely available software (Segment, Medviso AB) by two independent readers (GA and RT), each with more than five years of experience in CMR imaging. T1 values were measured in the myocardium, liver, spleen, skeletal muscle and the blood for the FCM group and in the myocardium and the blood pool for the gadobutrol group. All measurements were performed by manually drawing a region of interest (ROI) on the T1 maps. Myocardial T1 was measured in a mid-ventricular short-axis slice by placing a ROI in the mid-mural region of the interventricular septum, avoiding the endocardial and epicardial borders to minimize partial volume contamination from the blood pool. Blood T1 was assessed by drawing a ROI in the LV cavity blood pool, with care taken to avoid inclusion of the papillary muscles. T1 of liver, spleen and skeletal muscle was measured by manually drawing a ROI in each of the tissues. Fig. 2 shows an example of ROI placement in the different tissues. The partition coefficient lambda for a given contrast agent in the myocardium, liver, spleen or skeletal muscle was calculated as the ratio of ΔR1 of a given tissue over ΔR1 of the blood ($\lambda = \Delta R1_{tissue} / \Delta R1_{blood}$), where R1=1/T1 and ΔR1 is the difference in R1 between post- and pre-contrast [19].

Statistical analysis. Statistical analysis was performed using SPSS® software (version 24; IBM®, Somers, New York, USA) and Microsoft Excel® (Microsoft®, Redmond, Washington, USA). Continuous data are presented as mean ± standard deviation (SD) or mean ± standard error of the mean (SEM) as designated. T1 measurement

changes over time were tested using ANOVA. Differences between groups were tested using the Mann-Whitney U test, as appropriate. Statistical significance was defined as p-value < 0.05.

Results

A total of twenty-five healthy male volunteers were evaluated, eight subjects (age 27 ± 3 years, range 22-32 years) were included in the FCM group and seventeen subjects (age 27± 5 years, range 20-39 years) in the gadobutrol group. Baseline clinical and imaging characteristics of both groups are summarized in Table 1.

FCM group – T1 values and R1 changes. In the FCM group, T1 values in all measured tissues were significantly reduced 20 minutes after the onset of FCM infusion compared with pre-contrast T1 values: blood (1331±73 vs 1558±60 ms), myocardium (914±32 vs 978±30 ms), liver (535±47 vs 550±42 ms). Spleen (1005±71 vs 1095±66 ms), skeletal muscle (807±22 vs 854±27 ms, $p < 0.001$ for all). Detailed T1 measurements are provided in Supplementary Table S1. Representative native and post-contrast T1 maps are shown in Fig. 3. Correspondingly, R1 increased in all tissues at the 20-minute time point relative to baseline, resulting in a significant rise in ΔR1 for all tissues ($p < 0.001$ for all).

FCM group – partition coefficient (λ). The partition coefficient λ remained stable over time in the myocardium and spleen ($p = 0.29$ and $p = 0.25$ for trend, respectively), with values at 30 min after the onset of FCM administration of 65±2% and 81±20%, respectively. Indicating attainment of a dynamic equilibrium between blood and myocardium and spleen. In contrast, λ in the liver and skeletal muscle increased progressively over the 60-minute observation period ($p < 0.001$ for trend for both tissues), indicating that a dynamic equilibrium was not achieved in these organs. The temporal evolution of T1, R1, ΔR1 and λ across all tissues over 60-minute following FCM infusion is illustrated in Fig. 4.

Comparison with gadobutrol. T1 measurements in the myocardium and blood for the gadobutrol group are provided in Supplementary Table S2. Myocardial λ in the gadobutrol, measured 15-20 minutes after intravenous injection was 42±1%. Myocardial λ was significantly higher in the FCM group in the gadobutrol group (65±2 vs 42±1%, $p < 0.000$; Fig. 5).

Discussion

The main finding of the study is that T1 mapping can quantitatively measure the *in vivo* distribution of intravenously administered FCM into the myocardium, liver, spleen, skeletal muscle and blood. Furthermore, the myocardial distribution of FCM into the myocardium was substantially higher than for the extracellular agent gadobutrol, consistent with an additional intracellular distribution for FCM.

The observed increase in R1 across all measured tissues following FCM infusion is consistent with a previously reported animal study demonstrating a linear relationship between R1 and tissue iron concentration in the liver and myocardium [24]. FCM administration is known to initially promote the systemic release of iron from cells of the reticuloendothelial system into the blood circulation [25; 26]. The resulting rise in blood iron concentration observed here is in agreement with prior human pharmacokinetics data [27]. Notably, iron concentrations increased at markedly different rates among the measured tissues, reflecting tissue-specific differences in iron uptake kinetics. This is further supported by a prior human study reporting significant splenic T1 shortening markedly by day 14 following a single dose of intravenous injection of FCM, with partial recovery by day 42 [12].

The partition coefficient λ, defined as the ratio of the change in tissue R1 to the change in blood R1, provides a measure of the fractional distribution volume of a contrast agent between tissue and blood. A stable λ over time termed dynamic equilibrium [28] or equilibrium distribution [18]. This implies that the rate of exchange of contrast agent between the blood and tissue compartments exceeds the rate of change in blood contrast agent concentration. In the present study. λ remained constant in the myocardium and spleen over the 60-minute observation period (65±2% and 81±20%, respectively), indicating that dynamic equilibrium was achieved in these organs. In contrast, However, λ increased progressively in the liver and skeletal muscle, indicating ongoing accumulation of FCM without attainment of dynamic equilibrium. This is consistent with the known physiology of non-heme iron uptake, which proceeds via transferrin-bound [29] and non-transferrin-bound iron uptake such as through the divalent metal transporter 1 [30]. It may be that these mechanisms have a more drawn-out time course in the liver and skeletal muscle such that a dynamic equilibrium is not achieved during the first hour after intravenous administration. By comparison, in the setting of myocardial iron overload, the calcium channels have been suggested to be the main route of iron uptake into cardiomyocytes [31; 32]. Myocardial λ for FCM exceeded that for gadobutrol by a mean of 23 percentage points. Since gadobutrol, as a purely extracellular agent, distributes exclusively within the extracellular space, the markedly higher myocardial λ observed for FCM indicates

distribution beyond the extracellular compartment, implicating intracellular uptake as the principal additional mechanism. However. It should be acknowledged that alternative explanations including differences in myocardial iron relaxivity relative to gadolinium, partial intravascular protein binding of iron, or pharmacokinetic differences between agents affecting timing of λ measurements cannot be entirely excluded.

In light of a relatively new recommendation of iron therapy in heart failure patients [6], improved understanding of the iron physiology that contributes to improvement of cardiac function in these patients' group is of increasing importance. Quantification of myocardial λ of FCM by using T1 mapping may provide additional insight into the pathophysiology of heart failure and may provide more information on how the FCM influences myocardial function. However, further studies are required to evaluate the utility of T1 mapping for quantifying FCM in myocardium, specifically in patients with heart failure.

Limitations

This study has several limitations that warrant consideration. First, simultaneous T2* measurement were not obtained which has been shown to have an agreement with tissue iron content [33], and is more specific for iron using single time point measurements. However, a study by Sado et al. [14] demonstrated that T1 mapping may be more sensitive than T2* in quantification of myocardial iron overload and has a better reproducibility [14; 34]. Second, the two study groups employed different MOLLI sampling schemes, 5(3s)3 for the gadobutrol group and 4(1s)3(1s)2 for the FCM group, which may introduce a systematic difference in absolute T1 accuracy [35]. In addition, the gadobutrol cohort was recruited separately, rendering the between-group comparison indirect and potentially subject to residual confounding. However, this influence is likely negligible due to the calculation of the partition coefficient, which relies on relative rather than absolute R1 changes. Third, we acknowledge that the 60 minutes follow up was not have been sufficient to capture the dynamic equilibrium of FCM in the liver and skeletal muscle. However, exploring the potential dynamic equilibrium beyond 60 minutes was beyond the scope of this study. As demonstrated in the study by Beshara et al. (25), hepatic uptake of intravenous iron progresses gradually, reaching approximately 55% of administered iron by 3.5 hours and plateauing near 60% by 8 hours, highlighting the slower dynamic equilibrium in the liver. Finally, the sample size was modest, with imbalance between groups reflecting their separate recruitment context, nonetheless, the FCM group size was determined to be adequate for detecting changes in T1 values and partition coefficient with 80% power.

Conclusions

T1 mapping enables quantitative and dynamic characterization the in vivo distribution of intravenously administered FCM across the myocardium, liver, spleen and skeletal muscle. Notably, myocardial λ for FCM was markedly higher than the extracellular agent gadobutrol, indicating that FCM distributes to a greater extent into healthy myocardium, most likely reflecting additional distribution into the intracellular space. The present approach offers a non-invasive CMR framework for studying myocardial iron physiology in vivo, with potential application in both healthy subjects and patients with myocardial disease.

Abbreviations

CMR	Cardiovascular magnetic resonance
ECV	Extracellular volume
FCM	Ferric carboxymaltose
MOLLI	Modified Look-Locker inversion recovery
MRI	Magnetic resonance imaging
R1	Longitudinal relaxation rate (1/T1)

References

1 Sciatti E, Lombardi C, Ravera A et al (2016) Nutritional Deficiency in Patients with Heart Failure. Nutrients 8. https://doi.org/10.3390/nu8070442

2 Funk F, Ryle P, Canclini C, Neiser S, Geisser (2010) The new generation of intravenous iron: chemistry, pharmacology, and toxicology of ferric carboxymaltose. Arzneimittel-Forschung 60:345–353. https://doi.org/10.1055/s-0031-1296299

3 Ponikowski P, Kirwan BA, Anker SD et al (2020) Ferric carboxymaltose for iron deficiency at discharge after acute heart failure: a multicentre, double-blind, randomised, controlled trial. Lancet 396:1895–1904. https://doi.org/ 10.1016/S0140-6736(20)32339-4.

4 von Haehling S, Doehner W, Evertz R et al (2024) Ferric carboxymaltose and exercise capacity in heart failure with preserved ejection fraction and iron deficiency: the FAIR-HFpEF trial. European Heart Journal 45:3789–3800. https://doi.org/ 10.1093/eurheartj/ehae479

5 Anker SD, Comin Colet J, Filippatos G et al (2009) Ferric carboxymaltose in patients with heart failure and iron deficiency. New England Journal of Medicine 361:2436–2448. https://doi.org/ doi: 10.1056/NEJMoa0908355

6 Ponikowski P, van Veldhuisen DJ, Comin-Colet J et al (2015) Beneficial effects of long-term intravenous iron therapy with ferric carboxymaltose in patients with symptomatic heart failure and iron deficiencydagger. European Heart Journal 36:657–668. https://doi.org/ 10.1093/eurheartj/ehu385

7 Haddad S, Wang Y, Galy B et al (2017) Iron-regulatory proteins secure iron availability in cardiomyocytes to prevent heart failure. European Heart Journal 38:362–372. https://doi.org/ 10.1093/eurheartj/ehw333

8 Carpenter JP, He T, Kirk P et al (2014) Calibration of myocardial T2 and T1 against iron concentration. J Cardiovasc Magn Reson 16:62. https://doi.org/ 10.1186/s12968-014-0062-4
9 Anderson LJ, Holden S, Davis B et al (2001) Cardiovascular T2-star (T2*) magnetic resonance for the early diagnosis of myocardial iron overload. European Heart Journal 22:2171–2179. https://doi.org/ 10.1053/euhj.2001.2822
10 Zhang J, Chamberlain R, Etheridge M et al (2014) Quantifying iron-oxide nanoparticles at high concentration based on longitudinal relaxation using a three-dimensional SWIFT Look-Locker sequence. Magnetic Resonance in Medicine 71:1982–1988. https://doi.org/ 10.1002/mrm.25181
11 Núñez J, Miñana G, Cardells I et al (2020) Noninvasive Imaging Estimation of Myocardial Iron Repletion Following Administration of Intravenous Iron: The Myocardial-IRON Trial. J Am Heart Assoc 9:e014254. https://doi.org/ 10.1161/JAHA.119.014254
12 Vera-Aviles M, Kabir SN, Shah A et al (2024) Intravenous iron therapy results in rapid and sustained rise in myocardial iron content through a novel pathway. European Heart Journal 45:4497–4508. https://doi.org/10.1093/eurheartj/ehae359
13 Vera-Aviles M, Kabir SN, Shah A et al (2024) Intravenous iron therapy results in rapid and sustained rise in myocardial iron content through a novel pathway. Eur Heart J 45:4497–4508. https://doi.org/ 10.1093/eurheartj/ehae359
14 Sado DM, Maestrini V, Piechnik SK et al (2015) Noncontrast myocardial T1 mapping using cardiovascular magnetic resonance for iron overload. Journal of Magnetic Resonance Imaging 41:1505–1511. https://doi.org/ 10.1002/jmri.24727
15 Messroghli DR, Greiser A, Frohlich M, Dietz R, Schulz-Menger J (2007) Optimization and validation of a fully-integrated pulse sequence for modified look-locker inversion-recovery (MOLLI) T1 mapping of the heart. Journal of Magnetic Resonance Imaging 26:1081–1086. https://doi.org/10.1002/jmri.21119
16 Flett AS, Hayward MP, Ashworth MT et al (2010) Equilibrium contrast cardiovascular magnetic resonance for the measurement of diffuse myocardial fibrosis: preliminary validation in humans. Circulation 122:138–144.https://doi.org/10.1161/CIRCULATIONAHA.109.930636.
17 Schelbert EB, Testa SM, Meier CG et al (2011) Myocardial extravascular extracellular volume fraction measurement by gadolinium cardiovascular magnetic resonance in humans: slow infusion versus bolus. J Cardiovasc Magn Reson 13:16. https://doi.org/10.1186/1532-429X-13-16
18 Arheden H, Saeed M, Higgins CB et al (1999) Measurement of the distribution volume of gadopentetate dimeglumine at echo-planar MR imaging to quantify myocardial infarction: comparison with 99mTc-DTPA autoradiography in rats. Radiology 211:698–708. https://doi.org/10.1148/radiology.211.3.r99jn41698
19 Flacke SJ, Fischer SE, Lorenz CH (2001) Measurement of the gadopentetate dimeglumine partition coefficient in human myocardium in vivo: normal distribution and elevation in acute and chronic infarction. Radiology 218:703–710. https://doi.org/10.1148/radiology.218.3.r01fe18703
20 Nickander J, Themudo R, Thalén S et al (2019) The relative contributions of myocardial perfusion, blood volume and extracellular volume to native T1 and native T2 at rest and during adenosine stress in normal physiology. Journal of Cardiovascular Magnetic Resonance 21:73. https://doi.org/10.1186/s12968-019-0585-9
21 Liu S, Han J, Nacif MS et al (2012) Diffuse myocardial fibrosis evaluation using cardiac magnetic resonance T1 mapping: sample size considerations for clinical trials. J Cardiovasc Magn Reson 14:90. https://doi.org/10.1186/1532-429X-14-90
22 Kellman P, Arai AE, Xue H (2013) T1 and extracellular volume mapping in the heart: estimation of error maps and the influence of noise on precision. Journal of Cardiovascular Magnetic Resonance 15:56. https://doi.org/10.1186/1532-429X-15-56
23 Xue H, Shah S, Greiser A et al (2012) Motion correction for myocardial T1 mapping using image registration with synthetic image estimation. Magnetic Resonance in Medicine 67:1644–1655. https://doi.org/10.1002/mrm.23153
24 Wood JC, Otto-Duessel M, Aguilar M et al (2005) Cardiac iron determines cardiac T2*, T2, and T1 in the gerbil model of iron cardiomyopathy. Circulation 112:535–543. https://doi.org/10.1161/CIRCULATIONAHA.104.504415
25 Ding Y, Zhu X, Li X et al (2020) Pharmacokinetic, Pharmacodynamic, and Safety Profiles of Ferric Carboxymaltose in Chinese Patients with Iron-deficiency Anemia. Clinical Therapeutics 42:276–285. https://doi.org/10.1016/j.clinthera.2019.12.010

26 Geisser P (2009) The pharmacology and safety profile of ferric carboxymaltose (Ferinject®): structure/reactivity relationships of iron preparations. Port J Nephrol Hypert 23:11–16.
27 Beshara S, Sörensen J, Lubberink M et al (2003) Pharmacokinetics and red cell utilization of 52Fe/59Fe-labelled iron polymaltose in anaemic patients using positron emission tomography. British Journal of Haematology 120:853–859. https://doi.org/10.1046/j.1365-2141.2003.03590.x
28 Ugander M, Oki AJ, Hsu LY et al (2012) Extracellular volume imaging by magnetic resonance imaging provides insights into overt and sub-clinical myocardial pathology. European Heart Journal 33:1268–1278. https://doi.org/10.1093/eurheartj/ehr481
29 Aisen P (2004) Transferrin receptor 1. Int J Biochem Cell Biol 36:2137–2143. https://doi.org/
30 Gunshin H, Mackenzie B, Berger UV et al (1997) Cloning and characterization of a mammalian proton-coupled metal-ion transporter. Nature 388:482–488. https://doi.org/10.1038/41343
31 Kumfu S, Chattipakorn S, Srichairatanakool S, Settakorn J, Fucharoen S, Chattipakorn N (2011) T-type calcium channel as a portal of iron uptake into cardiomyocytes of beta-thalassemic mice. Eur J Haematol 86:156–166. https://doi.org/10.1111/j.1600-0609.2010.01549.x
32 Oudit GY, Sun H, Trivieri MG et al (2003) L-type Ca2+ channels provide a major pathway for iron entry into cardiomyocytes in iron-overload cardiomyopathy. Nat Med 9:1187–1194. https://doi.org/10.1038/nm920
33 Kirk P, He T, Anderson LJ et al (2010) International reproducibility of single breathhold T2* MR for cardiac and liver iron assessment among five thalassemia centers. Journal of Magnetic Resonance Imaging 32:315–319. https://doi.org/10.1002/jmri.22245
34 Krittayaphong R, Zhang S, Saiviroonporn P et al (2017) Detection of cardiac iron overload with native magnetic resonance T1 and T2 mapping in patients with thalassemia. International Journal of Cardiology 248:421–426. https://doi.org/10.1016/j.ijcard.2017.06.100
35 Kellman P, Hansen MS (2014) T1-mapping in the heart: accuracy and precision. Journal of Cardiovascular Magnetic Resonance 16:2. https://doi.org/10.1186/1532-429X-16-2

Figure captions

Fig. 1 Figure 1. Study population and main part of CMR protocol used for calculation of FCM and Gd lambda (λ). FCM, Ferric Carboxymaltose; Gd, gadolinium-based contrast agent, gadobutrol

Fig. 2 An example of regions of interest for T1 measurements made for each organ in a healthy volunteer. Note that the regions of interest for each organ were carefully placed to avoid partial volume

Fig. 3 A pre-contrast native T1 map (a), and post-contrast (b) (25 minutes after onset of intravenous injection of ferric carboxymaltose) short-axis T1 map in a mid-ventricular slice in a healthy volunteer. T1 maps are displayed using the same color scale as displayed on the right. Note how the post-contrast images have a visibly shorter T1, most prominent in the blood, but also present in the myocardium

Fig. 4 T1, R1, ΔR1 and the partition coefficient (lambda) of normal myocardium (black squares), liver (blue solid triangle), spleen (green solid circle), skeletal muscle (open diamond) and blood (red solid circles) over time after injection of ferric carboxymaltose in healthy volunteers (n=8). Note how lambda, which is the ratio of ΔR1 of a given tissue to ΔR1 of blood, remains constant over time for myocardium and the spleen, but not for the liver and skeletal muscle, up to 90 minutes after injection. Data are shown as mean values and error bars denote standard error of the mean

Fig. 5 Fractional distribution volume (lambda) of ferric carboxymaltose and gadobutrol in healthy myocardium Ferric carboxymaltose exhibited a markedly higher myocardial lambda than for the extracellular agent, gadobutrol ($P < 0.0001$), indicating higher myocardial distribution. Bars represent mean lambda and error bars denote standard error of the mean (SEM)

Table 1. Clinical and MRI characteristics of the study cohorts

	Ferric carboxymaltose	Gadobutrol	*P* value
Male sex, n/total (%)	8/8 (100)	17/17 (100)	n/a
Age, years	27±3	27±5	0.82
Height, cm	180±6	181±5	0.52
Weight, kg	81±13	79±9	0.59
BMI, kg/m^2	25.0±3.5	24.0±2.7	0.41
BSA, m^2	2.0±0.2	2.0±0.1	0.76
LV end-diastolic volume, ml	204±29	202±35	0.89
LV end-diastolic volume index, ml/m^2	101±13	101±15	0.97
LV end-systolic volume, ml	77±12	82±18	0.44
LV end-systolic volume index, ml/m^2	38±5	41±8	0.36
LV ejection fraction, %	62±3	59±4	0.08
LV mass, g	127±25	141±22	0.16
LV mass index, g/m^2	64±10	70±9	0.15

Data are shown as mean±SD or number (%). BMI, body mass index; BSA, body surface area; LV, Left ventricle

Author contributions

GA was involved in the study design, participant recruitment, obtained data, performed blinded assessments, contributed to data analysis, performed statistical analysis and drafted the manuscript. RT obtained data from gadolinium group and helped to edit the manuscript. ML, JN, PS and AS participated in manuscript editing. MU participated in the study design and manuscript editing. All authors reviewed and approved the final manuscript.

Funding

The research was funded in part by the Swedish Research Council, Swedish Heart and Lung Foundation, the Stockholm County Council, and Karolinska Institute.

Statements & Declarations

The authors declare no competing interests.

Ethics approval

The study is a prospective exploratory study of healthy male controls that received Institutional Review Board approval. Written informed consent was obtained from all subjects in this study.

Figures

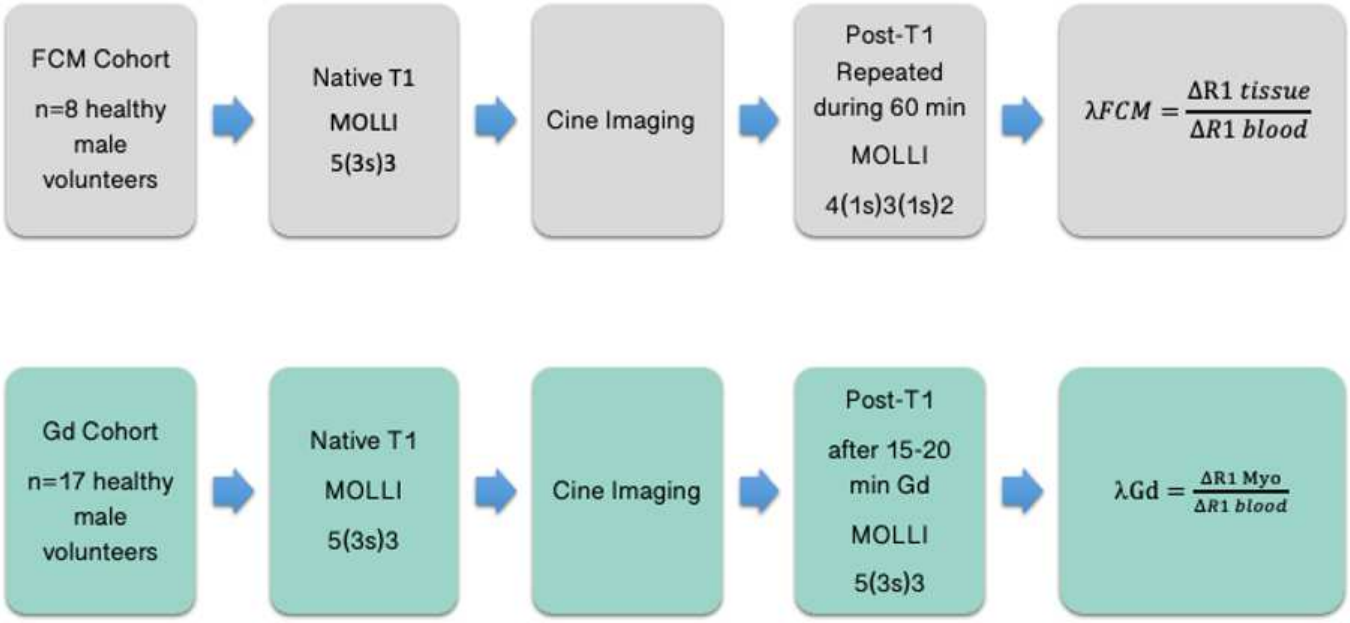


Figure 1

Study population and main part of CMR protocol used for calculation of FCM and Gd lambda (l). FCM, Ferric Carboxymaltose; Gd, gadolinium-based contrast agent, gadobutrol

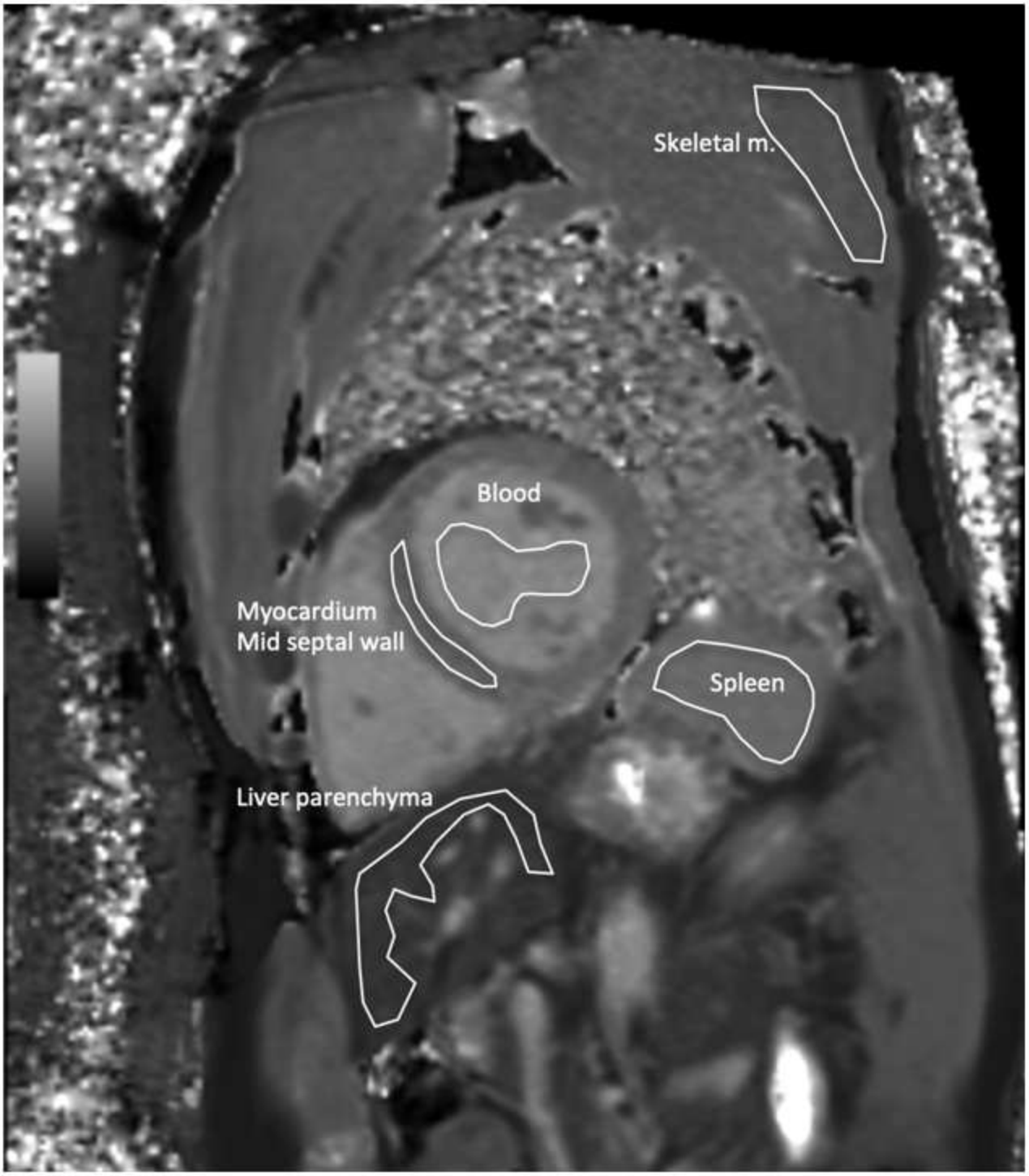


Figure 2

An example of regions of interest for T1 measurements made for each organ in a healthy volunteer. Note that the regions of interest for each organ were carefully placed to avoid partial volume

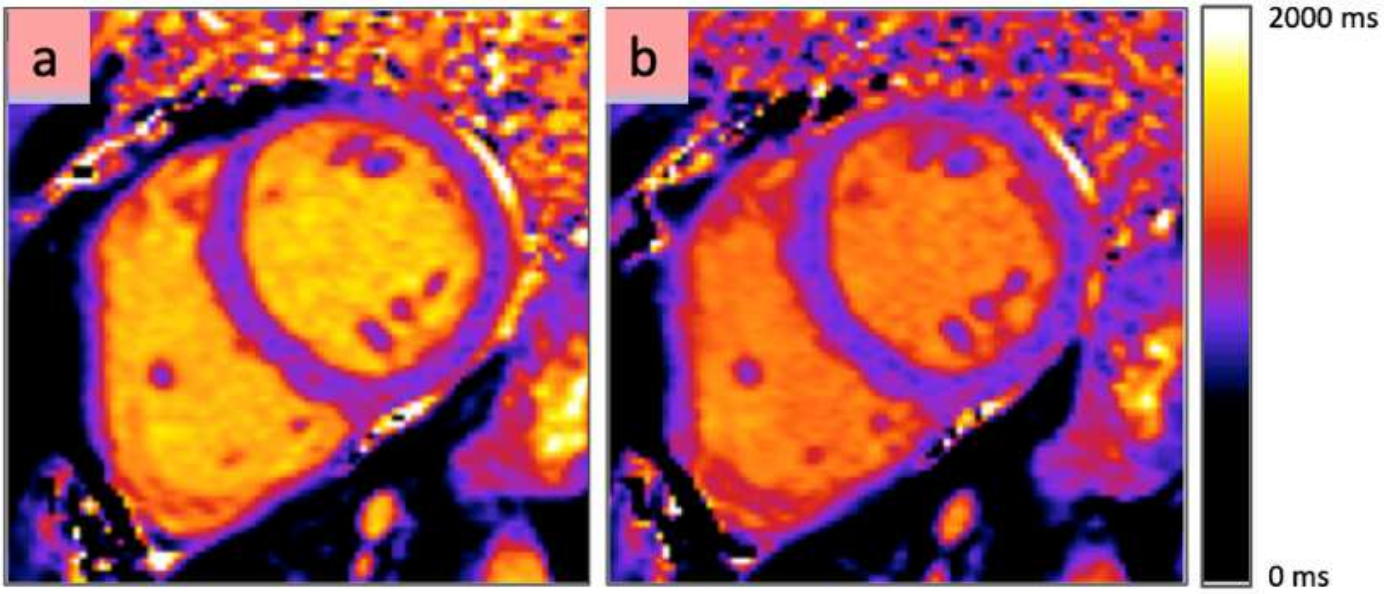


Figure 3

A pre-contrast native T1 map (a), and post-contrast (b) (25 minutes after onset of intravenous injection of ferric carboxymaltose) short-axis T1 map in a mid-ventricular slice in a healthy volunteer. T1 maps are displayed using the same color scale as displayed on the right. Note how the post-contrast images have a visibly shorter T1, most prominent in the blood, but also present in the myocardium

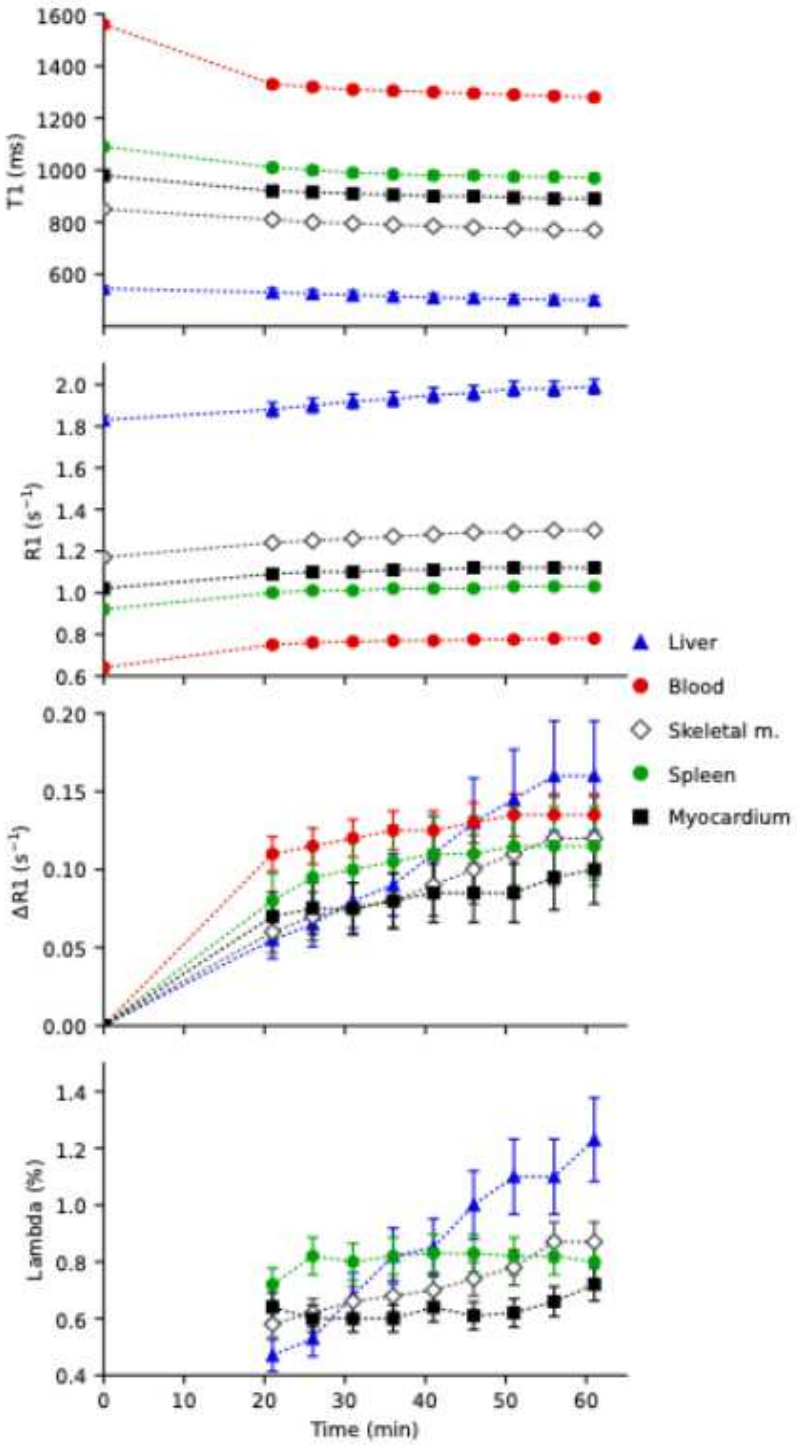


Figure 4

T1, R1, ΔR1 and the partition coefficient (lambda) of normal myocardium (black squares), liver (blue solid triangle), spleen (green solid circle), skeletal muscle (open diamond) and blood (red solid circles) over time after injection of ferric carboxymaltose in healthy volunteers (n=8). Note how lambda, which is the ratio of ΔR1 of a given tissue to ΔR1 of blood, remains constant over time for myocardium and the

spleen, but not for the liver and skeletal muscle, up to 60 minutes after injection. Data are shown as mean values and error bars denote standard error of the mean

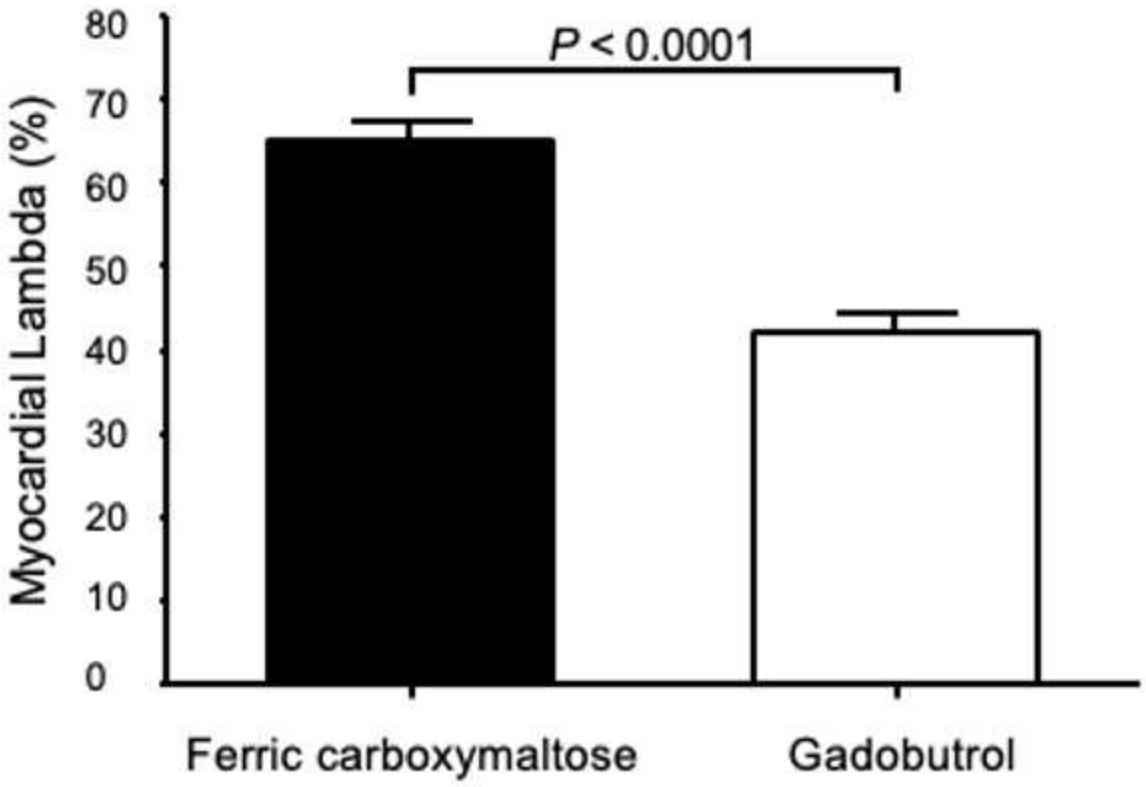


Figure 5

Fractional distribution volume (lambda) of ferric carboxymaltose and gadobutrol in healthy myocardium. Ferric carboxymaltose exhibited a markedly higher myocardial lambda than for the extracellular agent, gadobutrol (P < 0.0001), indicating higher myocardial distribution. Bars represent mean lambda and error bars denote standard error of the mean (SEM)

Supplementary Files

This is a list of supplementary files associated with this preprint. Click to download.

- SupplementarytableS1and2.T1measurementsinFCMcohort.docx